Temperature-Dependent Photoluminescence of ZnTe Films Grown on Si Substrates

2003 Chinese Phys. Lett. 20 2049

(http://iopscience.iop.org/0256-307X/20/11/042)

Temperature-Dependent Photoluminescence of ZnTe Films Grown on Si Substrates *

SHAN Chong-Xin(单崇新), FAN Xi-Wu(范希武), ZHANG Ji-Ying(张吉英), ZHANG Zhen-Zhong(张振中), LU You-Ming(吕有明), LIU Yi-Chun(刘益春), SHEN De-Zhen(申德振)

Key Laboratory of Excited State Processes, Changchun Institute of Optics, Fine Mechanics and Physics, Chinese Academy of Sciences, Changchun 130033

(Received 26 June 2003)

ZnTe films have been prepared on Si substrates by metal-organic chemical vapour deposition (MOCVD), and the temperature-dependent photoluminescence (PL) properties were investigated. The near-band-edge (NBE) emission of the ZnTe sample at 83 K shows an asymmetry line shape, which can be decomposed into two Gaussian lines labelled by FE and BE. Temperature-dependent PL intensity of the NBE peak shows two variation regions, and an expression with two dissociation channels fits well to the experimental data. The results of the temperature-dependent full width at half maximum (FWHM) and peak energy were well understood under the framework of the two-dissociation-channel model. That is, at low temperature, the emission from bound excitons governs the NBE peak, while above 157 K, the free exciton emission becomes dominant gradually. A simple model with three energy levels was employed to describe the variation in emission intensity of BE and FE with temperature.

PACS: 78. 55. Et, 78. 66. Hf, 81. 15. Gh

ZnTe is a wide band gap II-VI compound semiconductor with direct band-gap of 2.26 eV at room temperature. This material has a very large electro-optic coefficient, which is advantageous for applications to THz detectors, waveguide devices, modulators and light emitting device (LED) operated in the pure-green spectrum region.[1−3] However, just as ZnSe-base semiconductor compounds, long lifetime ZnTe LED has not been realized, although much attention has been paid. One of the impediments lies in the dissatisfaction with temperature characteristics and the rapid degradation process. Namely, the output degraded drastically at elevated operating temperature. Therefore, the study of temperature evolution characters of semiconductors, so as to make out the dissociation channels of excitons, is urgently important.[4−6] In particular, more attention should be paid to ZnTe grown on Si substrates for its possible integration with the mature Si-base microelectronic technology.[7] We have prepared ZnTe films on Si substrates with ZnO as a buffer layer in the previous literature.[8] In this Letter, we report temperature-dependent optical properties of the ZnTe film grown on silicon substrates, two dissociation channels of exciton were made out.

The preparation of ZnTe films in this study is carried out by two steps, a ZnO film with thickness of 800 nm was firstly sputtered onto a Si (111) substrate to obtain the ZnTe films with good structural and luminescent properties.[9] The sputtering of the ZnO layer was performed at 150°C in the gas mixture of Ar (75%) and O_2 (25%) by a reactive frequency sputtering equipment with a 99.99% zinc pellet as the Zn source. After that, the ZnO layer was annealed at 900°C in oxygen ambient for one hour to obtain a preferred orientation. A ZnTe layer with thickness of 800 nm was then deposited onto the ZnO buffered Si (111) substrate by low-pressure MOCVD at 420°C with the growth pressure of 220 Torr. Dimethylzinc (DMZn) and diethyltelluride (DETe) were employed as precursors of Zn and Te. The preparation process can also be found elsewhere.[8] The structural properties of the ZnTe film were accessed by a D/max-rA x-ray diffraction (XRD) spectrometer (Rigaku) with a Cu K_α line of 1.54 Å. For photoluminescence (PL) investigations, the 488-nm line of an Ar^+ laser was selected as the excitation source and the signals were recorded by the charge-coupled device of a JY-630 micro-Raman spectrograph designed specially for wide band gap semiconductors.

The structure property of the ZnTe film grown on the ZnO buffered Si (111) substrate was examined by XRD measurement. As shown in Fig. 1, three diffraction peaks were observed. The peak at 34.6° corresponds to ZnO (002), while the peaks at $2\theta = 25.2°$ and 49.8° correspond to the diffraction from (111) and (311) ZnTe. The XRD measurement indicates that the ZnTe film has a cubic structure with the (111) preferred orientation.

Figure 2 shows the PL spectrum of the investigated sample taken at 83 K. There appear four peaks including the NBE emission E and the deep level emissions I_1, I_2, and I_3. The enlarged plot of E is shown

* Supported by the Innovation Project of Chinese Academy of Sciences, the Hundred Talents Programme of Chinese Academy of Sciences, the National Natural Science Foundation of China under Grant Nos 69896260 and 60077015, and the National High Technology Research and Development Programme of China under Grant No 209AA31112.

in the inset of this figure. A prominent feature of peak E is the asymmetry of the broad lineshape. One can model peak E as a superposition of two Gaussian lines marked by BE and FE, as shown by the curves in the inset. The energy difference between BE and FE is 18.5 meV. FE is thought of as the emission from free excitons. Given the energy discrepancy, BE may be the emission from exciton bound to a neutral double acceptor, which may be group Ⅳ impurity, most likely, carbon introduced by the organic metal precursors.[10,11] For the origin of I_1, I_2 and I_3, according to their peak position, I_1 is known as the recombination of donor-acceptor pairs,[12] I_2 is the so-called Y band,[13] which is commonly observed in ZnTe[14,15] and other Ⅱ-Ⅵ semiconductors, such as ZnSe[16] and CdTe.[17] The peak of I_3, which is not fully displayed in the figure, is the emission from excitons bound to oxygen in the interface of the ZnTe and ZnO buffer layers.[18] The detailed description of I_1, I_2, and I_3 is beyond the investigation scope of this study. The temperature-dependent characteristics of peak E are studied in the following.

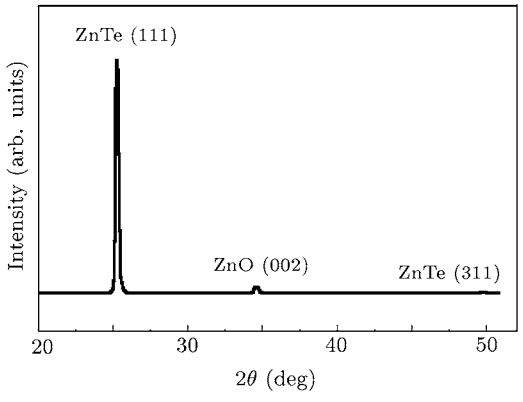

Fig. 1. XRD pattern of the ZnTe film grown on a ZnO-buffered Si (111) substrate.

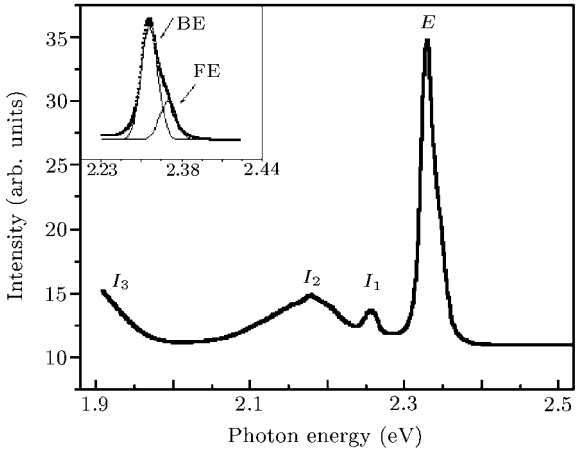

Fig. 2. PL spectrum of ZnTe/ZnO/Si at 83 K, the inset shows the two-line fit to peak E.

Data presented in Fig. 3(a) are the enlarged temperature-dependent PL spectra of peak E, and the integrated intensity of the asymmetry peak versus temperature is shown in Fig. 3(b). The dashed line in Fig. 3(a) denotes roughly the peak position of FE. As shown in the figure, there are clearly two temperature-dependent regions, one is from 83 to 157 K, and the other from 157 to 300 K. Assuming that there is a three-energy-level system with energies of $E_{A1} = E_1 - E_0$ and $E_{A2} = E_2 - E_0$, one can state the distribution of carriers among the ground E_0, the first excited state E_1 and the second excited state E_2 in the following form:[19]

$$N_0(T) + N_1(T) + N_2(T) = N_G(T), \tag{1}$$

$$N_1(T)/N_0(T) = (\alpha_1/\alpha_0)\exp\{-(E_1 - E_0)/K_BT\}, \tag{2}$$

$$N_2(T)/N_0(T) = (\alpha_2/\alpha_0)\exp\{-(E_2 - E_0)/K_BT\}, \tag{3}$$

where $N_0(T)$, $N_1(T)$ and $N_2(T)$ are the number of carriers in the energy levels of E_0, E_1 and E_2 at temperature of T; while α_0, α_1 and α_2 are the degenerations of the three energy levels, and $N_G(T)$ is the total carrier population in this system. The following formula can be derived based on the above three equations:

$$N_G(T) = N_0(T)[1 + (\alpha_1/\alpha_0)e^{-E_1-E_0)/K_BT} + (\alpha_2/\alpha_0)e^{-(E_2-E_0)/K_BT}]. \tag{4}$$

Taking that $N_G(T)$ is temperature-independent, that is, $N_G(T) = N_G(0) = N_0(0)$, we can rewrite Eq. (4) as

$$N_0(T) = \frac{N_G(0)}{1 + A_1\exp\left(\frac{-E_{A1}}{K_BT}\right) + A_2\exp\left(\frac{-E_{A2}}{K_BT}\right)}, \tag{5}$$

where $A_1 = \alpha_1/\alpha_0$, $A_2 = \alpha_2/\alpha_0$, $E_{A1} = E_1 - E_0$ and $E_{A2} = E_2 - E_0$. It is supposed that the radiative transition probability in the whole investigated temperature range is unchanged, the expression between emission intensity and temperature can be expressed in the following form:

$$I(T) = \frac{I_0}{1 + A_1\exp\left(\frac{-E_{A1}}{K_BT}\right) + A_2\exp\left(\frac{-E_{A2}}{K_BT}\right)}. \tag{6}$$

The solid curve in Fig. 3(b) is the theoretical fit to the integrated PL intensity by Eq. (6). Two activation energies obtained are $E_{A1} = 13.6$ meV and $E_{A2} = 19.3$ meV. Considering that the exciton binding energy in ZnTe is 13 meV,[20] which is close to the value of E_{A1}, one can then deduce that E_{A1} corresponds to the dissociation of free excitons. Since E_{A2} is almost equal to the energy difference of BE and FE, which is about 18.5 meV as mentioned above. Therefore, it is concluded that in the low temperature range from 83 to 157 K, the emission from BE governs the

peak E. With the increasing temperature, the BE will delocalize to become free excitons, and the emission from free excitons becomes dominant in the temperature range from 157 to 300 K.

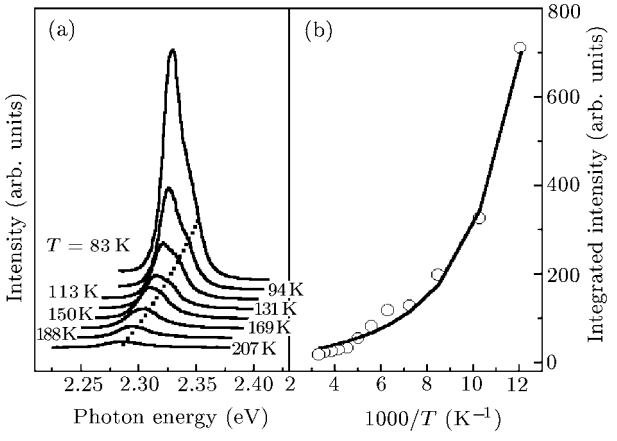

Fig. 3. (a) PL spectra of the investigated sample at different temperatures. (b) Integrated intensity and theoretical fit to the integrated intensity by $I(T) = I_0[1 + A_1 \exp(-E_{A1}/K_BT) + A_2 \exp(-E_{A2}/K_BT)]^{-1}$.

The dependence of FWHM of peak E on temperature is shown in Fig. 4, in which the scattered rectangles are the experimental data, and the solid curve is the theoretical simulation to the data. As illustrated by the experimental data, the line-width increases with temperature. However, there is a kink point at about 157 K, which is taken to originate from the impurity scattering, as detailed hereafter.

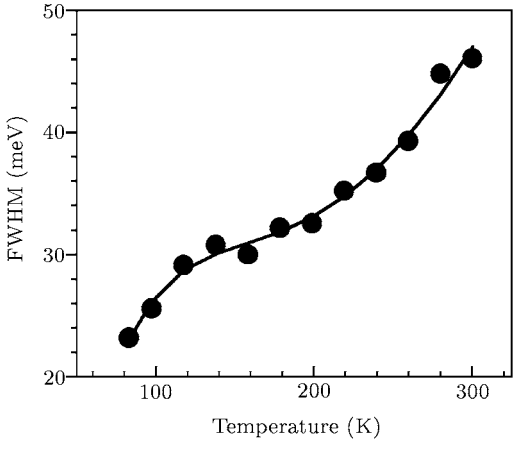

Fig. 4. Temperature-dependent FWHM of the ZnTe film. The dots show the experimental data and the curve is the fitting line to the experimental data by Eq. (7).

In general, the FWHM of an emission line is mainly contributed to by a temperature-independent component $\Gamma_{\rm inh}$ and a temperature-dependent homogeneous component Γ_h. The inhomogeneous part of $\Gamma_{\rm inh}$ mainly results from the nonuniformity in the epilayer, while the homogeneous component comprises three parts.[21] At low temperature, the scattering by longitudinal acoustic (LA) phonon dominates the broadening of the emission. At a moderate temperature, scattered by the longitudinal optical (LO) phonon becomes dominant due to increasing the phonon population. As the temperature increases further, the broadening due to impurity scattering has to be taken into account because of the ionization of some impurities. Based on the above depiction, the FWHM can be expressed as:[20,22,23]

$$\Gamma = \Gamma_{\rm inh} + \Gamma_{LA}T + \frac{\Gamma_{LO}}{\exp(E_{LO}/K_BT) - 1} + \frac{\Gamma_{\rm imp}}{\exp(E_{\rm imp}/K_BT)}, \quad (7)$$

where $\Gamma_{\rm inh}$ is the inhomogeneous broadening factor, Γ_{LA}, Γ_{LO} and $\Gamma_{\rm imp}$ are the measure weightings of the LA and LO phonon and impurity scattering, respectively. E_{LO} is the energy of LO phonon and $E_{\rm imp}$ is the ionization energy of exciton bound to impurity. K_B is the Boltzmann constant and T is the sample temperature. Considering that the LO phonon energy in ZnTe is 26.1 meV,[24] by fitting the experimental using Eq. (7), as shown by the curve in Fig. 4, one can obtain $E_{LO} = 25.7$ meV and $E_{\rm imp} = 17.4$ meV. The good accordance of the simulation curve to the experimental data indicates that the broadening caused by phonon scattering dominates the width of peak E at low temperature, while scattering by ionized impurity governs the width at high temperature (> 157).

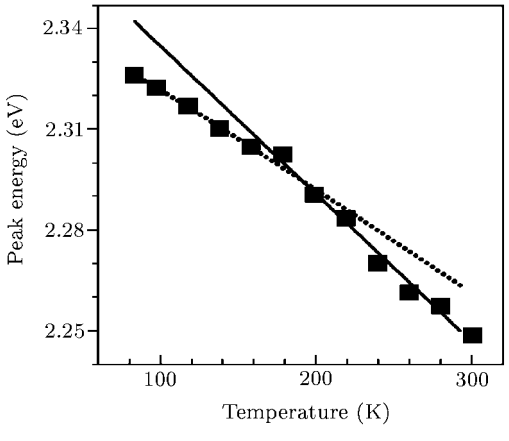

Fig. 5. Temperature dependence of the peak energy of the ZnTe film. The dotted line shows the fit to the experimental data from 83 K to 157 K and the solid line indicates the fit to the data from 157 K to 300 K using the Varshni equation.

The dependence of the emission peak energy of peak E on temperature is displayed in Fig. 5, in which solid squares denote the experimental data, the dotted line shows a theoretical fit to the data from 83 to 157 K, while the solid line indicates fit to data from

157 to 300 K using the Varshni equation:[25]

$$E_g(T) = E_g(0) - \frac{\alpha T^2}{T+\beta}, \tag{8}$$

where $E_g(0)$ is the peak energy at 0 K; α and β are the constants, and T is temperature. Since the emission spectrum in our experiment shows two-temperature-region characters, the temperature dependence peak energy of peak E was simulated in two regions accordingly. By fitting the data from 83 K to 157 K, one can obtain $E_g(0) = 2.363$ eV. In the same way, the value of $E_g(0)$ obtained by fitting the data from 157 to 300 K is 2.379 eV, taking the exciton binding energy into account, this value is in little difference from 2.39 eV, the reported band gap of ZnTe at 0 K.[26] The energy discrepancy between the two $E_g(0)$ values obtained from the different temperature ranges is 15.1 meV, which is close to the energy difference between FE and BE when the error is taken into account. The value of β obtained by fitting the experimental data above 157 K is -1.7 K. Moreover, the temperature coefficient of the peak energy obtained from fitting the experimental data above 157 K is 4.4×10^{-4} eV/K, which is almost the same as the reported 4.5×10^{-4} eV/K for free excitons emission in ZnTe.[22] This again confirms that the dissociation of exciton in our experiment has two channels. At low temperature, the bound exciton emission governs peak E, and the bound exciton was delocalized into free exciton as temperature increases. Consequently, the emission from free exciton dominates peak E at elevated temperature. It has to be admitted that the transition from bound exciton dominant emission to free exciton dominant one is a slow-going process, this may explain the experimental error in this study to some extent.

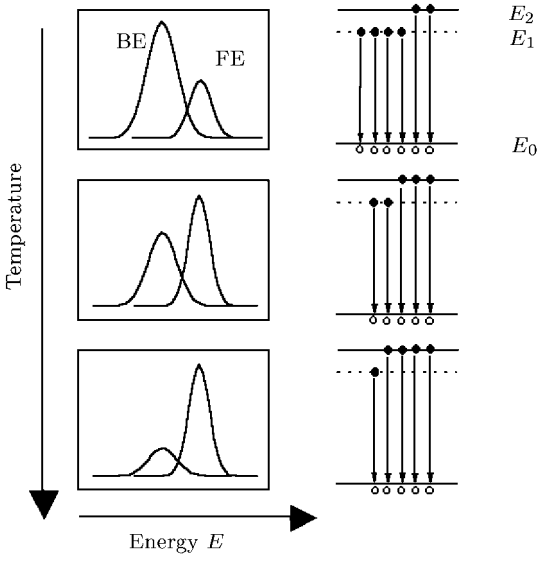

Fig. 6. Schematic model with two energy levels for the asymmetry emission peak evolution with the increasing temperature.

Based on the above analysis, The variation of BE and FE can be expressed by a three-level model put forward by Ko *et al.*,[27] as shown in Fig. 6. The recombination of E_2 to E_0 and E_1 to E_0 in this model denotes schematically the free and bound exciton emission in our experiment. At low temperature, the carrier population in E_1 prevails over that in E_2, thus the emission from bound excitons dominates the emission spectrum. As temperature rises, the carriers in E_1 can be excited onto E_2, namely the bound excitons are delocalized to become free excitons. Therefore, the emission from bound excitons decreases and that from free excitons becomes dominant.

In summary, temperature-dependent optical properties of ZnTe films grown on silicon substrates have been investigated. The near-band-edge emission of the investigated sample shows two components labelled by BE and FE. Based on the energy difference of these two components and the results of temperature-dependent emission intensity, the two radiative centres are attributed to free- and bound-exciton emissions, respectively. The variations of the emission FWHM and peak energy with temperature confirm this assignment. A simple model with three energy levels was employed to depict the relative variation in emission intensity of BE and FE with temperature.

References

[1] Chang J H et al 2001 *Appl. Phys. Lett.* **78** 566
[2] Chang J H et al 2000 *J. Vac. Sci. Technol.* B **18** 1530
[3] Sato K 2000 *Phys. Status Solidi* A **180** 267
[4] Pan Z et al 2001 *Chin. Phys. Lett.* **18** 659
[5] Wei Y Q et al 2001 *Chin. Phys. Lett.* **18** 982
[6] Liang X G et al 2002 *Chin. Phys. Lett.* **19** 1203
[7] Wang W S 1997 *Mater. Chem. Phys.* **51** 80
[8] Shan C X et al 2002 *J. Vac. Sci. Technol.* A **20** 1886
[9] Shan C X et al 2001 *J. Cryst. Growth* **233** 795
[10] Nagnea M et al 1983 *Solid State Commun.* **47** 703
[11] Tanaka T et al 2003 *J. Crystal Growth* 248 43
[12] Ekawa M and Taguchi T 1989 *Jpn. J. Appl. Phys.* Part II **28** L1341
[13] Yu Y M et al 2001 *J. Appl. Phys.* **90** 807
[14] Garica J A et al 1998 *J. Crystal Growth* **191** 685
[15] Gheyas S I et al 1996*Appl. Surf. Sci.* **100/101** 647
[16] Taguchi T et al 1985 *J. Crystal Growth* **72** 46
[17] Fujii S et al 1989 *Jpn. J. Appl. Phys.* Part II **28** 1712
[18] Ekawa M et al 1988 *J. Crystal Growth* **93** 667
[19] Bimberg D, Sondergeld M and Grobe E 1971 *Phys. Rev.* B **4** 3451
[20] Li T, Lozykowski H J and Reno J L 1992 *Phys. Rev.* B **46** 6961
[21] Wang S Z et al 2001 *J. Appl. Phys.* **90** 2314
[22] Yoshimura S et al 1995 *Jpn. J. Appl. Phys.* **34** 1459
[23] Lozykowski H J and Shastri V K 1991 *J. Appl. Phys.* **69** 3235
[24] Venghaus H and Dean P J 1980 *Phys. Rev.* B **21** 1596
[25] Varshni Y P 1967 *Physica* **34** 149
[26] Nahory R E and Fan H Y 1966 *Phys. Rev. Lett.* **17** 251
[27] Ko H C et al 1998 *Appl. Phys. Lett.* **73** 1388